# Analysis of dynamical behaviors of a double belt friction-oscillator model

Ge Chen
Shandong Normal University
School of Mathematical Sciences
Ji'nan, 250014
PR China
2179541091@qq.com

Jinjun Fan*
Shandong Normal University
School of Mathematical Sciences
Ji'nan, 250014
PR China
fjj18@126.com

*Abstract:* In this paper, analytical results of complex motions of a double belt friction-oscillator are investigated using the flow switchability theory of the discontinuous dynamical systems. The friction-oscillator is composed of a mass connected by viscoelastic element and linear spring-loading and interacting with two moving belts by means of dry friction. Different domains and boundaries for such system are defined according to the friction discontinuity, which exhibits multiple discontinuous boundaries in the phase space. The necessary and sufficient conditions of the stick motions, non-stick motions and grazing motions of such system are given in the form of theorem mathematically. The switching planes and basic mappings will be defined to study grazing motions and periodic motions. The results of computer simulation of the stick motions and grazing motions for different parameters are submitted in the present paper. With appropriate mapping structures, the simulation of the stick and non-stick periodic motions for such an oscillator are also given.

*Key–Words:* double belt friction-oscillator; discontinuous dynamical system; switchability; stick motion; grazing motion

## 1 Introduction

Discontinuous dynamical systems exist everywhere in engineering [1-13]. In mechanical engineering, most of the dynamical systems are discontinuous. One used to adopt continuous models for approximate descriptions of discontinuous dynamical systems. However, such continuous modeling cannot provide adequate predictions of discontinuous dynamical systems, and also makes the problems solving be more complicated and inaccurate. To better describe the real world, one should realize that discontinuous models can provide adequate and real predications of engineering systems. Therefore, a theory applicable to discontinuous dynamical systems should be built.

The early study of discontinuous dynamical systems goes back to Den Hartog [1] in 1931. Den Hartog considered a forced oscillator with Coulomb and viscous damping. In 1960, Levitan [2] investigated a friction oscillator with the periodically driven base, and also discussed the stability of the periodic motion. In 1966, Masri and Caughey [3] discussed a discontinuous impact damper, and obtained the stability of the symmetrical period-1 motion of the impact damper. More detailed discussions on the general motion of impact dampers were also developed in Masri [4]. In 1976, Utkin [5] first investigated

the controlled dynamical systems in view of discontinuity. This method is called sliding mode control. Utkin [6] applied the sliding mode control in variable structure systems, and more detailed theory of this method was also developed in [7] by Utkin. In 1986, Shaw [8] investigated the non-stick periodic motion of a dry-friction oscillator, and discussed the stability of this motion through the Poincare mapping. In 1988, Filippov [9] investigated the dynamic behaviors of a Coulomb friction oscillator and developed differential equations with discontinuous right-hand sides. The analytical conditions of sliding motion along the discontinuous boundary were developed through differential inclusion, and the existence and uniqueness of the solution were also discussed. Leine etal. [10] investigated the stick-slip vibration induced by an alternate friction models through the shooting method in 1998. In 1999, Galvanetto and Bishop [11] discussed dynamics of a simple dynamical system subjected to an elastic restoring force, viscous damping and dry friction forces and studied the non-standard bifurcations with analytical and numerical tools. Pilipchuk and Tan [12] studied the friction induced vibration of a two-degree-of-freedom friction oscillator in 2004. In 2005, Casini and Vestroni [13] investigated dynamics of two double-belt friction oscillators by means of

analytical and numerical tools.

However, the dynamical behaviors of discontinuous dynamical system is stilled difficult to investigate. Luo [14-19] developed a general theory for discontinuous dynamical systems and gave its applications in engineering. The G-functions for discontinuous dynamical systems are the mail tools to investigate singularity in discontinuous dynamical systems and introduced by Luo [17] in 2008 and further developed on time-varying domains by Luo [18] in 2009. Based on the G-functions, the full and half sink and source, non-passable flows to the separation boundary in discontinuous dynamical systems were discussed, and the necessary and sufficient conditions of the switching bifurcations between the passable and non-passable flows were presented. The detailed discussion can be referred to Luo [19]. Based on this theory, lots of discontinuous models can be investigated easily, for example [20 − 26].

In this paper, analytical conditions for stick, non-stick and grazing motions of the double-belt friction oscillator will be developed using the flow switchability theory of the discontinuous dynamical systems. Different domains and boundaries for such system are defined according to the friction discontinuity, which exhibits multiple discontinuous boundaries in the phase space. Based on the above domains and boundaries, the analytical conditions of the stick motions and grazing motions are obtained mathematically. The switching planes and basic mappings will be defined to study grazing motions and periodic motions. For a better understanding of the dynamical behaviors, the numerical simulations are given to illustrate the analytical results of the complex motions.
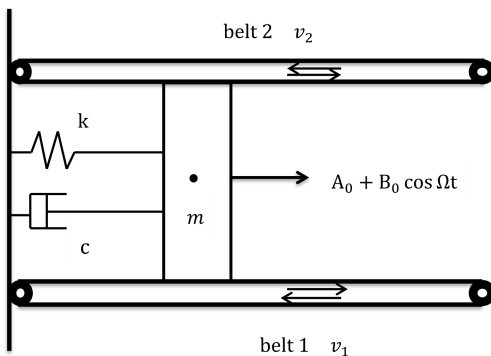
## 2 Physical Model



Figure 1: Physical model

Consider a periodically forced oscillator, attached

to a fixed wall, as shown in Fig. 1. This friction-induced oscillator includes a mass $m$, a spring of stiffness $k$ and a damper of viscous damping coefficient $c$. In this configuration, the mass $m$ is continuously in contact with both belts which are pushed onto the mass with a constant forced $F_N$ and possess the same friction characteristics. The periodic driving force $A_0 + B_0 \cos \Omega t$ exerts on the mass, where $A_0$, $B_0$ and $\Omega$ are the constant force, excitation strength and frequency ratio, respectively.

Since the mass contacts the moving belts with friction, the mass can move along or rest on the belt 1 or belt 2 surface. Further, a kinetic friction force shown in Fig. 2 is described as

$$F_f(\dot{x}) \begin{cases} = (\mu_1 + \mu_2)F_N, & \dot{x} \in [\,v_2, +\infty), \\ \in [(\mu_1 - \mu_2)F_N, (\mu_1 + \mu_2)F_N], & \dot{x} = v_2, \\ = (\mu_1 - \mu_2)F_N, & \dot{x} \in [\,v_1, v_2\,], \\ \in [-(\mu_1 + \mu_2)F_N, (\mu_1 - \mu_2)F_N], & \dot{x} = v_1, \\ = -(\mu_1 + \mu_2)F_N, & \dot{x} \in (-\infty, v_1\,], \end{cases}$$
$$(1)$$

where $\dot{x} := dx/dt$, $F_N$ and $\mu_k (k = 1, 2)$ are a normal force to the contact surface and friction coefficients between the mass $m$ and the belt $k$ $(k = 1, 2)$, respectively. Here we assume that $v_2 > v_1$ and $\mu_1 \geq \mu_2$.
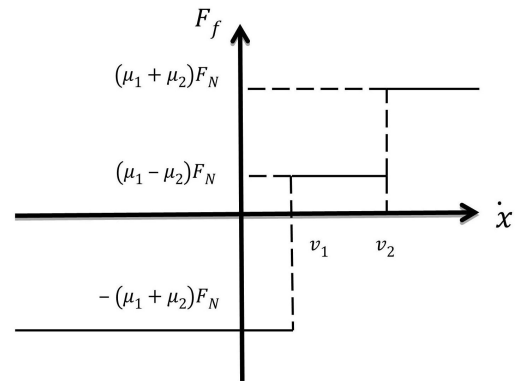


Figure 2: Friction force

The motions of the mass in a double-belt friction oscillator can be divided into two cases. If the mass moves along belt 1 and belt 2, the corresponding motion is called the non-stick motion. If the mass moves together with belt 1 or belt 2, the corresponding motion is called the stick motion.

For the mass moving with the same speed of the belt 1 surface, the force acting on the mass in the $x$-direction is defined as

$$F_{s1} = A_0 + B_0 \cos \Omega t - kx - c\dot{x} + \mu_2 F_N \text{ for } \dot{x} = v_1.$$
$$(2)$$

If this force cannot overcome the friction force $\mu_1 F_N$ (i.e., $|F_{s1}| \leq \mu_1 F_N$), the mass does not have any rel-

ative motion to the belt 1. The equation of the motion for the mass in such state is described as

$$\dot{x} = v_1, \qquad \ddot{x} = 0. \tag{3}$$

For the mass moving with the same speed of the belt 2 surface, we can also obtain the equation for the mass as follows

$$\dot{x} = v_2, \qquad \ddot{x} = 0. \tag{4}$$

For the non-stick motions of the friction-induced oscillator, we can obtain the equations of the motions as follows

$$\begin{cases} m\ddot{x} = A_0 + B_0 \cos \Omega t - kx - c\dot{x} + (\mu_1 + \mu_2)F_N \\ \qquad\qquad\qquad\qquad \text{for } \dot{x} < v_1, \\ m\ddot{x} = A_0 + B_0 \cos \Omega t - kx - c\dot{x} - (\mu_1 - \mu_2)F_N \\ \qquad\qquad\qquad\qquad \text{for } v_1 < \dot{x} < v_2, \\ m\ddot{x} = A_0 + B_0 \cos \Omega t - kx - c\dot{x} - (\mu_1 + \mu_2)F_N \\ \qquad\qquad\qquad\qquad \text{for } \dot{x} > v_2. \end{cases} \tag{5}$$

# 3 Domains and Boundaries

From the previous discussion, there are five motion states including three non-stick motions in the three regions and two stick motions on the boundaries. The phase plane can be partitioned into three domains and two boundaries, as shown in Fig. 3. In each domain, the motion can be described through a continuous dynamical system.
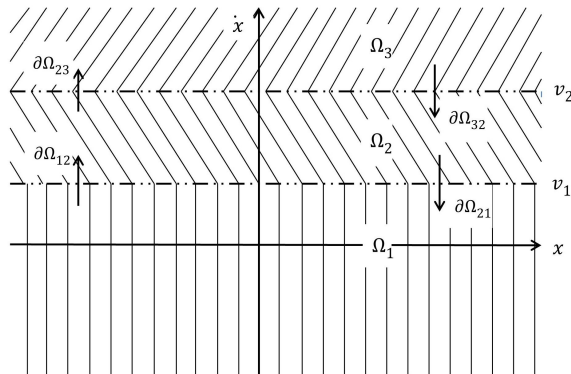


Figure 3: Domains and boundaries

The three domains are expressed by $\Omega_\alpha (\alpha = 1, 2, 3)$:

$$\Omega_1 = \Big\{ (x, \dot{x}) \,|\, x \in (-\infty, +\infty), \ \dot{x} \in (-\infty, v_1) \Big\},$$

$$\Omega_2 = \Big\{ (x, \dot{x}) \,|\, x \in (-\infty, +\infty), \ \dot{x} \in (v_1, v_2) \Big\},$$

$$\Omega_3 = \Big\{ (x, \dot{x}) \,|\, x \in (-\infty, +\infty), \ \dot{x} \in (v_2, +\infty) \Big\}. \tag{6}$$

The corresponding boundaries are defined as:

$$\partial\Omega_{12} = \partial\Omega_{21} = \Big\{ (x, \dot{x}) \,|\, x \in (-\infty, +\infty), \ \dot{x} = v_1 \Big\},$$

$$\partial\Omega_{23} = \partial\Omega_{32} = \Big\{ (x, \dot{x}) \,|\, x \in (-\infty, +\infty), \ \dot{x} = v_2 \Big\}. \tag{7}$$

Based on the above domains and boundaries, the vectors for motions of the mass in the domains can be introduced as follows

$$\mathbf{x}_{(\lambda)} = (x_{(\lambda)}, \dot{x}_{(\lambda)})^{\mathrm{T}}, \qquad \mathbf{F}_{(\lambda)} = (\dot{x}_{(\lambda)}, F_{(\lambda)})^{\mathrm{T}}, \tag{8}$$

where $\lambda = 1, 2, 3$ and

$$F_{(1)}(\mathbf{x}_{(1)}, t) = -\frac{c}{m}\dot{x}_{(1)} - \frac{k}{m}x_{(1)} + \frac{B_0}{m}\cos \Omega t$$
$$+ \frac{1}{m}[A_0 + (\mu_1 + \mu_2)F_N],$$

$$F_{(2)}(\mathbf{x}_{(2)}, t) = -\frac{c}{m}\dot{x}_{(2)} - \frac{k}{m}x_{(2)} + \frac{B_0}{m}\cos \Omega t$$
$$+ \frac{1}{m}[A_0 - (\mu_1 - \mu_2)F_N],$$

$$F_{(3)}(\mathbf{x}_{(3)}, t) = -\frac{c}{m}\dot{x}_{(3)} - \frac{k}{m}x_{(3)} + \frac{B_0}{m}\cos \Omega t$$
$$+ \frac{1}{m}[A_0 - (\mu_1 + \mu_2)F_N]. \tag{9}$$

From (5), the equations of the non-stick motions for the mass are rewritten in the vector form of

$$\dot{\mathbf{x}}_{(\lambda)} = \mathbf{F}_{(\lambda)}(\mathbf{x}_{(\lambda)}, t) \quad \text{for} \quad \lambda \in \{1, 2, 3\}. \tag{10}$$

For the stick motion, the equations of the motion for the mass are rewritten in the vector form of

$$\dot{\mathbf{x}}_{(\lambda)}^{(0)} = \mathbf{F}_{(\lambda)}^{(0)}(\mathbf{x}_{(\lambda)}, t) \quad \text{for} \quad \lambda \in \{1, 2\} \tag{11}$$

and

$$F_{(\lambda)}^{(0)}(\mathbf{x}_{(\lambda)}^{(0)}, t) = 0, \tag{12}$$

where

$$\mathbf{x}_{(\lambda)}^{(0)} = (x_{(\lambda)}^{(0)}, \dot{x}_{(\lambda)}^{(0)})^{\mathrm{T}}, \qquad \mathbf{F}_{(\lambda)}^{(0)} = (v_\lambda, F_{(\lambda)}^{(0)})^{\mathrm{T}}.$$

# 4 Analytical Conditions

By the theory of the flow switchability to a specific boundary in discontinuous dynamical system in [17], the switching conditions of the passability, stick motions and grazing flows of the double-belt friction oscillator will be developed in this section.

For convenience, we first introduce some concepts and several lemmas in flow switching theory.

Consider a discontinuous dynamical system

$$\dot{\mathbf{x}}^{(\alpha)} \equiv \mathbf{F}^{(\alpha)}(\mathbf{x}^{(\alpha)}, t, \mathbf{P}_\alpha) \in R^n \qquad (13)$$

in domain $\Omega_\alpha (\alpha = i, j)$ which has a flow $\mathbf{x}_t^{(\alpha)} = \mathbf{\Phi}(t_0, \mathbf{x}_0^{(\alpha)}, \mathbf{P}_\alpha, t)$ with an initial condition $(t_0, \mathbf{x}_0^{(\alpha)})$, and on the boundary

$$\partial\Omega_{ij} = \Big\{ \mathbf{x} \mid \varphi_{ij}(\mathbf{x}, t, \lambda) = 0,$$

$$\varphi_{ij} \text{ is } C^r - \text{continuous } (r \geq 1) \Big\} \subset R^{n-1},$$
$$(14)$$

there is a flow $\mathbf{x}_t^{(0)} = \mathbf{\Phi}(t_0, \mathbf{x}_0^{(0)}, \lambda, t)$ with an initial condition $(t_0, \mathbf{x}_0^{(0)})$. The 0-order $G$-functions of the flow $\mathbf{x}_t^{(\alpha)}$ to the flow $\mathbf{x}_t^{(0)}$ on the boundary in the normal direction of the boundary $\partial\Omega_{ij}$ are defined as

$$G_{\partial\Omega_{ij}}^{(\alpha)}(\mathbf{x}_t^{(0)}, t_\pm, \mathbf{x}_{t_\pm}^{(\alpha)}, \mathbf{P}_\alpha, \lambda)$$
$$\equiv G_{\partial\Omega_{ij}}^{(0,\alpha)}(\mathbf{x}_t^{(0)}, t_\pm, \mathbf{x}_{t_\pm}^{(\alpha)}, \mathbf{P}_\alpha, \lambda)$$
$$= D_{\mathbf{x}_t^{(0)}}{}^t\mathbf{n}_{\partial\Omega_{ij}}^T \cdot (\mathbf{x}_{t_\pm}^{(\alpha)} - \mathbf{x}_t^{(0)})$$
$$+ {}^t\mathbf{n}_{\partial\Omega_{ij}}^T \cdot (\dot{\mathbf{x}}_{t_\pm}^{(\alpha)} - \dot{\mathbf{x}}_t^{(0)}). \qquad (15)$$

The 1-order $G$-functions for a flow $\mathbf{x}_t^{(\alpha)}$ to a boundary flow $\mathbf{x}_t^{(0)}$ in the normal direction of the boundary $\partial\Omega_{ij}$ are defined as

$$G_{\partial\Omega_{ij}}^{(1,\alpha)}(\mathbf{x}_t^{(0)}, t_\pm^{(\alpha)}, \mathbf{x}_{t_\pm}^{(\alpha)}, \mathbf{P}_\alpha, \lambda)$$
$$= D_{\mathbf{x}_t^{(0)}}^2{}^t\mathbf{n}_{\partial\Omega_{ij}}^T \cdot (\mathbf{x}_{t_\pm}^{(\alpha)} - \mathbf{x}_t^{(0)})$$
$$+ 2D_{\mathbf{x}_t^{(0)}}{}^t\mathbf{n}_{\partial\Omega_{ij}}^T \cdot (\dot{\mathbf{x}}_{t_\pm}^{(\alpha)} - \dot{\mathbf{x}}_t^{(0)})$$
$$+ {}^t\mathbf{n}_{\partial\Omega_{ij}}^T \cdot (\ddot{\mathbf{x}}_{t_\pm}^{(\alpha)} - \ddot{\mathbf{x}}_t^{(0)}), \qquad (16)$$

where the total derivative

$$D_{\mathbf{x}_t^{(0)}}(\cdot) := \frac{\partial(\cdot)}{\partial\mathbf{x}_t^{(0)}} \cdot \dot{\mathbf{x}}_t^{(0)} + \frac{\partial(\cdot)}{\partial t},$$

the normal vector of the boundary surface $\partial\Omega_{ij}$ at point $\mathbf{x}^{(0)}(t)$ is given by

$$ {}^t\mathbf{n}_{\partial\Omega_{ij}}^T(\mathbf{x}^{(0)}, t, \lambda) = \triangledown\varphi_{ij}(\mathbf{x}^{(0)}, t, \lambda)$$
$$= \Big( \frac{\partial\varphi_{ij}}{\partial x_1^{(0)}}, \frac{\partial\varphi_{ij}}{\partial x_2^{(0)}}, \cdots, \frac{\partial\varphi_{ij}}{\partial x_n^{(0)}} \Big)^T \Big|_{(t, \mathbf{x}^{(0)})}, \qquad (17)$$

and $t_\pm = t \pm 0$.

If the flow $\mathbf{x}_t^{(\alpha)}$ contacts with the boundary at the time $t_m$, that is $\mathbf{x}_{t_m}^{(\alpha)} = \mathbf{x}_m = \mathbf{x}_{t_m}^{(0)}$, and the boundary $\partial\Omega_{ij}$ is linear, independent of time $t$, we have

$$G_{\partial\Omega_{ij}}^{(0,\alpha)}(\mathbf{x}_m, t_m, \mathbf{P}_\alpha, \lambda)$$
$$:= G_{\partial\Omega_{ij}}^{(0,\alpha)}(\mathbf{x}_{t_m}^{(0)}, t_{m\pm}, \mathbf{x}_{t_{m\pm}}^{(\alpha)}, \mathbf{P}_\alpha, \lambda)$$
$$= {}^t\mathbf{n}_{\partial\Omega_{ij}}^T \cdot \dot{\mathbf{x}}_t^{(\alpha)} \Big|_{(\mathbf{x}_m, t_{m\pm})}, \qquad (18)$$

$$G_{\partial\Omega_{ij}}^{(1,\alpha)}(\mathbf{x}_m, t_m, \mathbf{P}_\alpha, \lambda)$$
$$:= G_{\partial\Omega_{ij}}^{(1,\alpha)}(\mathbf{x}_{t_m}^{(0)}, t_{m\pm}, \mathbf{x}_{t_{m\pm}}^{(\alpha)}, \mathbf{P}_\alpha, \lambda)$$
$$= {}^t\mathbf{n}_{\partial\Omega_{ij}}^T \cdot \ddot{\mathbf{x}}_t^{(\alpha)} \Big|_{(\mathbf{x}_m, t_{m\pm})}. \qquad (19)$$

Here $t_{m+}$ and $t_{m-}$ are the time before approaching and after departing the corresponding boundary, respectively.

**Lemma 1** [17] *For a discontinuous dynamical system $\dot{\mathbf{x}}^{(\alpha)} = \mathbf{F}^{(\alpha)}(\mathbf{x}^{(\alpha)}, t, \mathbf{P}_\alpha) \in R^n$, $\mathbf{x}(t_m) = \mathbf{x}_m \in \partial\Omega_{ij}$ at time $t_m$. For an arbitrarily small $\varepsilon > 0$, there is a time interval $[t_{m-\varepsilon}, t_m)$. Suppose $\mathbf{x}^{(i)}(t_{m-}) = \mathbf{x}_m = \mathbf{x}^{(j)}(t_{m-})$. Both flows $\mathbf{x}^{(i)}(t)$ and $\mathbf{x}^{(j)}(t)$ are $C^r_{[t_{m-\varepsilon}, t_m)}$-continuous $(r \geq 1)$ for time $t$, and $\|d^{r+1}\mathbf{x}^{(\alpha)}/dt^{r+1}\| < \infty$ $(\alpha \in \{i, j\})$. The necessary and sufficient conditions for a sliding motion on $\partial\Omega_{\alpha\beta}$ are*

$$\left.\begin{matrix} G_{\partial\Omega_{ij}}^{(0,\alpha)}(\mathbf{x}_m, t_{m-}, \mathbf{P}_\alpha, \lambda) < 0 \\[2mm] G_{\partial\Omega_{ij}}^{(0,\beta)}(\mathbf{x}_m, t_{m-}, \mathbf{P}_\beta, \lambda) > 0 \end{matrix}\right\} \text{ for } \quad \mathbf{n}_{\partial\Omega_{\alpha\beta}} \to \Omega_\alpha, \qquad (20)$$

*where $\alpha, \beta \in \{i, j\}$ and $\alpha \neq \beta$.*

**Lemma 2** [17] *For a discontinuous dynamical system $\dot{\mathbf{x}}^{(\alpha)} = \mathbf{F}^{(\alpha)}(\mathbf{x}^{(\alpha)}, t, \mathbf{P}_\alpha) \in R^n$, $\mathbf{x}(t_m) = \mathbf{x}_m \in \partial\Omega_{ij}$ at time $t_m$. For an arbitrarily small $\varepsilon > 0$, there are two time intervals $[t_{m-\varepsilon}, t_m)$ and $(t_m, t_{m+\varepsilon}]$. Suppose $\mathbf{x}^{(i)}(t_{m-}) = \mathbf{x}_m = \mathbf{x}^{(j)}(t_{m+})$. Both flows $\mathbf{x}^{(i)}(t)$ and $\mathbf{x}^{(j)}(t)$ are $C^r_{[t_{m-\varepsilon}, t_m)}$ and $C^r_{(t_m, t_{m+\varepsilon}]}$-continuous $(r \geq 1)$ for time $t$, respectively, and $\|d^{r+1}\mathbf{x}^{(\alpha)}/dt^{r+1}\| < \infty$ $(\alpha \in \{i, j\})$. The flow $\mathbf{x}^{(i)}(t)$ and $\mathbf{x}^{(j)}(t)$ to the boundary $\partial\Omega_{ij}$ is semi-passable from domain $\Omega_i$ to $\Omega_j$ iff*

$$either \quad \left.\begin{matrix} G_{\partial\Omega_{ij}}^{(0,i)}(\mathbf{x}_m, t_{m-}, \mathbf{P}_i, \lambda) > 0 \\[2mm] G_{\partial\Omega_{ij}}^{(0,j)}(\mathbf{x}_m, t_{m+}, \mathbf{P}_j, \lambda) > 0 \end{matrix}\right\} for\ \mathbf{n}_{\partial\Omega_{\alpha\beta}} \to \Omega_j, \qquad (21)$$

$$
\left.
\begin{aligned}
& G^{(0,i)}_{\partial\Omega_{ij}}(\mathbf{x}_m, t_{m-}, \mathbf{P}_i, \lambda) < 0 \\
or \\
& G^{(0,j)}_{\partial\Omega_{ij}}(\mathbf{x}_m, t_{m+}, \mathbf{P}_j, \lambda) < 0
\end{aligned}
\right\} for\ \mathbf{n}_{\partial\Omega_{\alpha\beta}} \to \Omega_i.
$$
(22)

**Lemma 3** [17] *For a discontinuous dynamical system $\dot{\mathbf{x}}^{(\alpha)} = \mathbf{F}^{(\alpha)}(\mathbf{x}^{(\alpha)}, t, \mathbf{P}_\alpha) \in R^n$, $\mathbf{x}(t_m) = \mathbf{x}_m \in \partial\Omega_{ij}$ at time $t_m$. For an arbitrarily small $\varepsilon > 0$, there is a time interval $[t_{m-\varepsilon}, t_{m+\varepsilon}]$. Suppose $\mathbf{x}^{(\alpha)}(t_{m\pm}) = \mathbf{x}_m$. The flow $\mathbf{x}^{(\alpha)}(t)$ is $C^r_{[t_{m-\varepsilon}, t_{m+\varepsilon}]}$-continuous ($r_\alpha \geq 2$) for time $t$, and $\|d^{r+1}\mathbf{x}^{(\alpha)}/dt^{r+1}\| < \infty$ ($\alpha \in \{i, j\}$). A flow $\mathbf{x}^{(\alpha)}(t)$ in $\Omega_\alpha$ is tangential to the boundary $\partial\Omega_{ij}$ iff*

$$
G^{(0,\alpha)}_{\partial\Omega_{ij}}(\mathbf{x}_m, t_m, \mathbf{P}_\alpha, \lambda) = 0 \quad for \quad \alpha \in \{i, j\}; \quad (23)
$$

$$
\left.
\begin{aligned}
& either\ G^{(1,\alpha)}_{\partial\Omega_{ij}}(\mathbf{x}_m, t_m, \mathbf{P}_\alpha, \lambda) < 0\ for\ \mathbf{n}_{\partial\Omega_{\alpha\beta}} \to \Omega_\beta, \\
& or \quad G^{(1,\alpha)}_{\partial\Omega_{ij}}(\mathbf{x}_m, t_m, \mathbf{P}_\alpha, \lambda) > 0\ for\ \mathbf{n}_{\partial\Omega_{\alpha\beta}} \to \Omega_\alpha,
\end{aligned}
\right\}
$$
(24)

*where $\alpha, \beta \in \{i, j\}$ and $\alpha \neq \beta$.*

More detailed theory on the flow switchability such as high-order $G$-functions, the definitions or theorems about various flow passability in discontinuous dynamical systems can be referred to [17] and [19].

From the aforementioned definitions and lemmas, we give the analytical conditions for the flow switching in the double-belt friction oscillator.

For the double-belt friction oscillator in Section 2, the normal vectors of the boundaries $\partial\Omega_{12}$ and $\partial\Omega_{23}$ are given as

$$
\mathbf{n}_{\partial\Omega_{12}} = \mathbf{n}_{\partial\Omega_{21}} = (0, 1)^{\mathrm{T}}, \ \mathbf{n}_{\partial\Omega_{23}} = \mathbf{n}_{\partial\Omega_{32}} = (0, 1)^{\mathrm{T}}.
$$
(25)

The $G$-functions for such friction oscillator are simplified as $G^{(0,\alpha)}_{\partial\Omega_{ij}}(\mathbf{x}_{(\alpha)}, t_{m\pm})$ or $G^{(1,\alpha)}_{\partial\Omega_{ij}}(\mathbf{x}_{(\alpha)}, t_{m\pm})$.

**Theorem 4** *For the double-belt friction oscillator described in Section 2, we have the following results:*

(i) *The stick motion on $\mathbf{x}_m \in \partial\Omega_{12}$ at time $t_m$ appears iff the following conditions can be obtained:*

$$
F_{(1)}(\mathbf{x}_m, t_{m-}) > 0 \ and \ F_{(2)}(\mathbf{x}_m, t_{m-}) < 0. \quad (26)
$$

(ii) *The stick motion on $\mathbf{x}_m \in \partial\Omega_{23}$ at time $t_m$ appears iff the following conditions can be obtained:*

$$
F_{(2)}(\mathbf{x}_m, t_{m-}) > 0 \ and \ F_{(3)}(\mathbf{x}_m, t_{m-}) < 0. \quad (27)
$$

**Proof:** From the aforementioned definitions, the 0-order $G$-functions for the stick boundaries $\partial\Omega_{12}$ and $\partial\Omega_{23}$ in the double-belt friction oscillator are

$$
\begin{aligned}
& G^{(0,1)}_{\partial\Omega_{12}}(\mathbf{x}_m, t_{m\pm}) = \mathbf{n}^{\mathrm{T}}_{\partial\Omega_{12}} \cdot \mathbf{F}_{(1)}(\mathbf{x}_m, t_{m\pm}), \\
& G^{(0,2)}_{\partial\Omega_{12}}(\mathbf{x}_m, t_{m\pm}) = \mathbf{n}^{\mathrm{T}}_{\partial\Omega_{12}} \cdot \mathbf{F}_{(2)}(\mathbf{x}_m, t_{m\pm}),
\end{aligned}
$$
(28)

and

$$
\begin{aligned}
& G^{(0,2)}_{\partial\Omega_{23}}(\mathbf{x}_m, t_{m\pm}) = \mathbf{n}^{\mathrm{T}}_{\partial\Omega_{23}} \cdot \mathbf{F}_{(2)}(\mathbf{x}_m, t_{m\pm}), \\
& G^{(0,3)}_{\partial\Omega_{23}}(\mathbf{x}_m, t_{m\pm}) = \mathbf{n}^{\mathrm{T}}_{\partial\Omega_{23}} \cdot \mathbf{F}_{(3)}(\mathbf{x}_m, t_{m\pm}).
\end{aligned}
$$
(29)

From (25), the Eqs. (28) and (29) can be computed as:

$$
\begin{aligned}
& G^{(0,1)}_{\partial\Omega_{12}}(\mathbf{x}_m, t_{m-}) = F_{(1)}(\mathbf{x}_m, t_{m-}), \\
& G^{(0,2)}_{\partial\Omega_{12}}(\mathbf{x}_m, t_{m-}) = F_{(2)}(\mathbf{x}_m, t_{m-}),
\end{aligned}
$$
(30)

and

$$
\begin{aligned}
& G^{(0,2)}_{\partial\Omega_{23}}(\mathbf{x}_m, t_{m-}) = F_{(2)}(\mathbf{x}_m, t_{m-}), \\
& G^{(0,3)}_{\partial\Omega_{23}}(\mathbf{x}_m, t_{m-}) = F_{(3)}(\mathbf{x}_m, t_{m-}).
\end{aligned}
$$
(31)

By Lemma 1, the stick motion on $\mathbf{x}_m \in \partial\Omega_{12}$ at time $t_m$ appears iff

$$
G^{(0,1)}_{\partial\Omega_{12}}(\mathbf{x}_{(m)}, t_{m-}) > 0 \ and \ G^{(0,2)}_{\partial\Omega_{12}}(\mathbf{x}_{(m)}, t_{m-}) < 0,
$$
(32)

i.e.

$$
F_{(1)}(\mathbf{x}_m, t_{m-}) > 0 \ and \ F_{(2)}(\mathbf{x}_m, t_{m-}) < 0. \quad (33)
$$

Therefore, (i) holds. Similarly, (ii) holds.     $\square$

**Theorem 5** *For the double-belt friction oscillator described in Section 2, we have the following results:*

(i) *The non-stick motion (or called passable motion to boundary) on $\mathbf{x}_m \in \partial\Omega_{12}$ at time $t_m$ appears iff the following condition can be obtained:*

$$
F_{(1)}(\mathbf{x}_m, t_{m\pm}) \times F_{(2)}(\mathbf{x}_m, t_{m\mp}) > 0. \quad (34)
$$

(ii) *The non-stick motion on $\mathbf{x}_m \in \partial\Omega_{23}$ at time $t_m$ appears iff the following condition can be obtained:*

$$
F_{(2)}(\mathbf{x}_m, t_{m\pm}) \times F_{(3)}(\mathbf{x}_m, t_{m\mp}) > 0. \quad (35)
$$

**Proof:** By Lemma 2, passable motion on the boundary $\mathbf{x}_m \in \partial\Omega_{12}$ at time $t_m$ appears iff

$$G^{(0,1)}_{\partial\Omega_{12}}(\mathbf{x}_m, t_{m\pm}) \times G^{(0,2)}_{\partial\Omega_{12}}(\mathbf{x}_m, t_{m\mp}) > 0. \qquad (36)$$

By (25), we obtain

$$G^{(0,1)}_{\partial\Omega_{12}}(\mathbf{x}_m, t_{m\pm}) = F_{(1)}(\mathbf{x}_m, t_{m\pm}),$$
$$G^{(0,2)}_{\partial\Omega_{12}}(\mathbf{x}_m, t_{m\mp}) = F_{(2)}(\mathbf{x}_m, t_{m\mp}). \qquad (37)$$

Then (36) and (37) implies that (i) holds. The proof for (ii) is similar. $\qquad\square$

**Theorem 6** *For the double-belt friction oscillator described in Section* 2, *we have the following results:*

(i) *The grazing motion on* $\mathbf{x}_m \in \partial\Omega_{12}$ *at time* $t_m$ *appears iff the following conditions can be obtained:*

$$F_{(\alpha)}(\mathbf{x}_m, t_{m\pm}) = 0 \quad \text{for} \quad \alpha \in \{1,2\}, \qquad (38)$$

*if* $\alpha = 1$,

$$\nabla F_{(\alpha)}(\mathbf{x}_m, t_{m\pm}) \cdot \mathbf{F}_{(\alpha)}(\mathbf{x}_m, t_{m\pm}) + \frac{\partial F_{(\alpha)}(\mathbf{x}_m, t_{m\pm})}{\partial t_m} < 0, \qquad (39)$$

*if* $\alpha = 2$,

$$\nabla F_{(\alpha)}(\mathbf{x}_m, t_{m\pm}) \cdot \mathbf{F}_{(\alpha)}(\mathbf{x}_m, t_{m\pm}) + \frac{\partial F_{(\alpha)}(\mathbf{x}_m, t_{m\pm})}{\partial t_m} > 0. \qquad (40)$$

(ii) *The grazing motion on* $\mathbf{x}_m \in \partial\Omega_{23}$ *at time* $t_m$ *appears iff the following conditions can be obtained:*

$$F_{(\alpha)}(\mathbf{x}_m, t_{m\pm}) = 0 \quad \text{for} \quad \alpha \in \{2,3\}, \qquad (41)$$

*if* $\alpha = 2$,

$$\nabla F_{(\alpha)}(\mathbf{x}_m, t_{m\pm}) \cdot \mathbf{F}_{(\alpha)}(\mathbf{x}_m, t_{m\pm}) + \frac{\partial F_{(\alpha)}(\mathbf{x}_m, t_{m\pm})}{\partial t_m} < 0, \qquad (42)$$

*if* $\alpha = 3$,

$$\nabla F_{(\alpha)}(\mathbf{x}_m, t_{m\pm}) \cdot \mathbf{F}_{(\alpha)}(\mathbf{x}_m, t_{m\pm}) + \frac{\partial F_{(\alpha)}(\mathbf{x}_m, t_{m\pm})}{\partial t_m} > 0. \qquad (43)$$

**Proof:** By Lemma 3, the sufficient and necessary conditions for the grazing flows on the boundary $\partial\Omega_{12}$ are

$$G^{(0,\alpha)}_{\partial\Omega_{12}}(\mathbf{x}_m, t_{m\pm}) = 0 \quad \text{for} \quad \alpha \in \{1,2\}, \qquad (44)$$

$$G^{(1,1)}_{\partial\Omega_{12}}(\mathbf{x}_m, t_{m\pm}) < 0, \ G^{(1,2)}_{\partial\Omega_{12}}(\mathbf{x}_m, t_{m\pm}) > 0. \qquad (45)$$

From (25), (28) and (29), we have

$$\begin{aligned}
G^{(0,\alpha)}_{\partial\Omega_{12}}(\mathbf{x}_m, t_{m\pm}) &= \mathbf{n}^{\mathrm{T}}_{\partial\Omega_{12}} \cdot \mathbf{F}_{(\alpha)}(\mathbf{x}_m, t_{m\pm}) \\
&= F_{(\alpha)}(\mathbf{x}_m, t_{m\pm}) \quad \text{for } \alpha \in \{1,2\}.
\end{aligned}$$
$$(46)$$

From (19), we obtain

$$G^{(1,1)}_{\partial\Omega_{12}}(\mathbf{x}_m, t_{m\pm}) = \mathbf{n}^{\mathrm{T}}_{\partial\Omega_{12}} \cdot D_{\mathbf{x}^{(0)}_{t_m}} \mathbf{F}_{(1)}(\mathbf{x}_m, t_{m\pm})$$
$$= (0,1) \cdot D_{\mathbf{x}^{(0)}_{t_m}} \left( \dot{\mathbf{x}}_{(1)}, F_{(1)}(\mathbf{x}_m, t) \right)^{\mathrm{T}} \bigg|_{(\mathbf{x}_m, t_{m\pm})}$$
$$= \nabla F_{(1)}(\mathbf{x}_m, t_{m\pm}) \cdot \mathbf{F}_{(1)}(\mathbf{x}_m, t_{m\pm}) + \frac{\partial F_{(1)}(\mathbf{x}_m, t_{m\pm})}{\partial t_m}. \qquad (47)$$

Similarly,

$$G^{(1,2)}_{\partial\Omega_{12}}(\mathbf{x}_m, t_{m\pm})$$
$$= \nabla F_{(2)}(\mathbf{x}_m, t_{m\pm}) \cdot \mathbf{F}_{(2)}(\mathbf{x}_m, t_{m\pm}) + \frac{\partial F_{(2)}(\mathbf{x}_m, t_{m\pm})}{\partial t_m}. \qquad (48)$$

From (46),(47) and (48), (i) holds. In a similar manner, (ii) holds. $\qquad\square$

## 5  Switching Planes and Mappings

The switching planes are introduced as ($\lambda = 1, 2$):

$$\begin{aligned}
\Sigma^0_{(\lambda)} &= \{(x_i, \dot{x}_i, \Omega t_i) | \dot{x}_i = v_\lambda\}, \\
\Sigma^1_{(\lambda)} &= \{(x_i, \dot{x}_i, \Omega t_i) | \dot{x}_i = v^-_\lambda\}, \\
\Sigma^2_{(\lambda)} &= \{(x_i, \dot{x}_i, \Omega t_i) | \dot{x}_i = v^+_\lambda\},
\end{aligned}$$
$$(49)$$

where $v^-_\lambda = \lim_{\delta\to 0}(v_\lambda - \delta)$ and $v^+_\lambda = \lim_{\delta\to 0}(v_\lambda + \delta)$ for arbitrary small $\delta > 0$. Therefore, eight basic mappings will be defined as:

$$\begin{aligned}
P_1 &: \Sigma^0_{(1)} \to \Sigma^0_{(1)}, & P_2 &: \Sigma^1_{(1)} \to \Sigma^1_{(1)}, \\
P_3 &: \Sigma^2_{(1)} \to \Sigma^2_{(1)}, & P_4 &: \Sigma^0_{(2)} \to \Sigma^0_{(2)}, \\
P_5 &: \Sigma^1_{(2)} \to \Sigma^1_{(2)}, & P_6 &: \Sigma^2_{(2)} \to \Sigma^2_{(2)}, \\
P_7 &: \Sigma^1_{(2)} \to \Sigma^2_{(1)}, & P_8 &: \Sigma^2_{(1)} \to \Sigma^1_{(2)}.
\end{aligned}$$
$$(50)$$

In phase plane, the trajectories of mappings $P_\lambda$ ($\lambda \in \{2,3,5,6,7,8\}$) in $\Omega_\alpha$ ($\alpha \in \{1,2,3\}$) starting and ending at the velocity boundaries and stick mappings $P_\lambda(\lambda = 1, 4)$ are illustrated in Fig. 4.
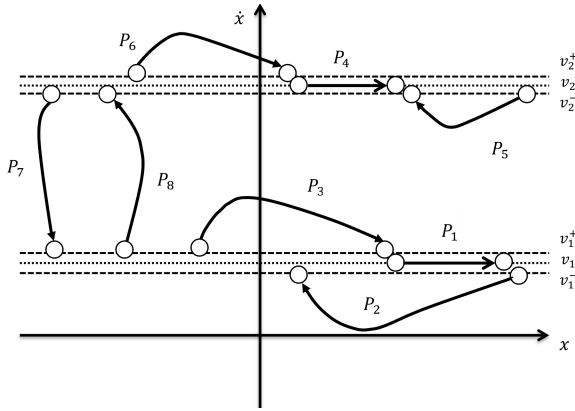
Figure 4: Basic mappings

From foregoing (49) and (50), we obtain

$$
\begin{aligned}
P_1: &\quad (x_i, v_1, \Omega t_i) \rightarrow (x_{i+1}, v_1, \Omega t_{i+1}), \\
P_2: &\quad (x_i, v_1^-, \Omega t_i) \rightarrow (x_{i+1}, v_1^-, \Omega t_{i+1}), \\
P_3: &\quad (x_i, v_1^+, \Omega t_i) \rightarrow (x_{i+1}, v_1^+, \Omega t_{i+1}), \\
P_4: &\quad (x_i, v_2, \Omega t_i) \rightarrow (x_{i+1}, v_2, \Omega t_{i+1}), \\
P_5: &\quad (x_i, v_2^-, \Omega t_i) \rightarrow (x_{i+1}, v_2^-, \Omega t_{i+1}), \\
P_6: &\quad (x_i, v_2^+, \Omega t_i) \rightarrow (x_{i+1}, v_2^+, \Omega t_{i+1}), \\
P_7: &\quad (x_i, v_2^-, \Omega t_i) \rightarrow (x_{i+1}, v_1^+, \Omega t_{i+1}), \\
P_8: &\quad (x_i, v_1^+, \Omega t_i) \rightarrow (x_{i+1}, v_2^-, \Omega t_{i+1}).
\end{aligned}
\tag{51}
$$

With (11) and (12), the governing equations for $P_\lambda (\lambda = 1, 4)$ can be described as

$$
\begin{cases}
x_{i+1} = v_1(t_{i+1} - t_i) + x_i, \\
A_0 + B_0 \cos \Omega t_{i+1} - k x_{i+1} - c v_1 + \mu_2 F_N = \mu_1 F_N,
\end{cases}
\tag{52}
$$

$$
\begin{cases}
x_{i+1} = v_2(t_{i+1} - t_i) + x_i, \\
A_0 + B_0 \cos \Omega t_{i+1} - k x_{i+1} - c v_2 - \mu_1 F_N = \mu_2 F_N,
\end{cases}
\tag{53}
$$

respectively.

For the double-belt friction oscillator, the domains $\Omega_\alpha$ ($\alpha \in \{1,2,3\}$) are unboubded. From the basic theorems of discontinuous dynamical system, only three possible bounded motions exist in the three domains. In domain $\Omega_\alpha$ ($\alpha \in \{1,2,3\}$), the displacement expressions and velocity expressions of the mass can be solved from (9) and (10). Using the displacement expressions and velocity expressions of the mass in domain $\Omega_\alpha$ ($\alpha \in \{1,2,3\}$), the governing equations of mapping $P_\lambda$ ($\lambda \in \{2,3,5,6,7,8\}$) are obtained. With (51), the governing equations of each mapping $P_\lambda$ ($\lambda \in \{2,3,5,6,7,8\}$) can be expressed

as

$$
f_1^{(\lambda)}(x_i, \Omega t_i, x_{i+1}, \Omega t_{i+1}) = 0,
$$
$$
f_2^{(\lambda)}(x_i, \Omega t_i, x_{i+1}, \Omega t_{i+1}) = 0.
\tag{54}
$$

The grazing motion occurs when a flow in a domain is tangential to the boundary and then returns back to this domain. The analytical conditions for the grazing motion in the double-belt friction oscillator were described as Lemma 3 and Theorem 6. If the grazing motion occurs at $(\mathbf{x}_m, t_m) \in \partial \Omega_{\alpha\beta}$ ($\alpha, \beta \in \{1,2\}$ or $\{2,3\}, \alpha \neq \beta$), more detailed theorem on the grazing motions will be developed.

For the double belt friction oscillator described in Section 2, there are four cases of grazing motions on the boundaries: the flow in domain $\Omega_1$ tangential to the boundary $\partial \Omega_{12}$, the flow in domain $\Omega_2$ tangential to the boundary $\partial \Omega_{21}$, the flow in domain $\Omega_2$ tangential to the boundary $\partial \Omega_{23}$, and the flow in domain $\Omega_3$ tangential to the boundary $\partial \Omega_{32}$, corresponding to the mapping $P_2$, $P_3$, $P_5$ and $P_6$, respectively. With (54), we can obtain the following theorem.

**Theorem 7** *For the double-belt friction oscillator described in Section 2, there are four kinds of grazing motions:*

(i) *Suppose the flow in domain $\Omega_1$ reaches $\mathbf{x}_m \in \partial \Omega_{12}$ at time $t_m$, the grazing motion on the boundary $\partial \Omega_{12}$ appears (i.e. the mapping $P_2$ is tangential to the boundary $\partial \Omega_{12}$) iff*

$$
\left.
\begin{aligned}
&\mathrm{mod}(\Omega t_m, 2\pi) \in [\,0, \pi + |\Theta_2^{\mathrm{cr}}|\,) \cup (\,2\pi - |\Theta_2^{\mathrm{cr}}|, 2\pi\,] \\
&\qquad\qquad\qquad\qquad for\ 0 < \gamma_2 < \tfrac{B_0}{m}\Omega; \\
&\mathrm{mod}(\Omega t_m, 2\pi) \in [\,0, \tfrac{3}{2}\pi\,) \cup (\,\tfrac{3}{2}\pi, 2\pi\,] \\
&\qquad\qquad\qquad\qquad for\ 0 < \gamma_2 = \tfrac{B_0}{m}\Omega; \\
&\mathrm{mod}(\Omega t_m, 2\pi) \in [\,0, 2\pi\,] \\
&\qquad\qquad\qquad\qquad for\ 0 < \tfrac{B_0}{m}\Omega < \gamma_2; \\
&\mathrm{mod}(\Omega t_m, 2\pi) \in (\,0, \pi\,) \\
&\qquad\qquad\qquad\qquad for\ \gamma_2 = 0; \\
&\mathrm{mod}(\Omega t_m, 2\pi) \in (\,\Theta_2^{\mathrm{cr}}, \pi - \Theta_2^{\mathrm{cr}}) \subset (\,0, \pi\,) \\
&\qquad\qquad for\ \gamma_2 < 0\ and\ \tfrac{B_0}{m}\Omega > |\gamma_2|; \\
&\mathrm{mod}(\Omega t_m, 2\pi) \in \{\varnothing\} \\
&\qquad\qquad for\ \gamma_2 < 0\ and\ \tfrac{B_0}{m}\Omega < |\gamma_2|,
\end{aligned}
\right\}
\tag{55}
$$

*where*

$$
\Theta_2^{\mathrm{cr}} = \arcsin(-\frac{\gamma_2 m}{B_0 \Omega}),
$$

*and*

$$
\gamma_2 = \frac{c}{m}\ddot{x}_{(1)}(t_m) + \frac{k}{m}\dot{x}_{(1)}(t_m).
$$

(ii) *Suppose the flow in domain $\Omega_2$ reaches $\mathbf{x}_m \in \partial \Omega_{21}$ at time $t_m$, the grazing motion on the boundary $\partial \Omega_{21}$ appears (i.e. the mapping $P_3$ is*

*tangential to the boundary $\partial\Omega_{21}$) iff*

$$
\left.\begin{array}{l}
\mathrm{mod}(\Omega t_m, 2\pi) \in (\,\pi + |\Theta_3^{\mathrm{cr}}|, 2\pi - |\Theta_3^{\mathrm{cr}}|\,) \subset (\,\pi, 2\pi) \\
\qquad\qquad\qquad\qquad \text{for } 0 < \gamma_3 < \frac{B_0}{m}\Omega; \\
\mathrm{mod}(\Omega t_m, 2\pi) \in \{\varnothing\} \\
\qquad\qquad\qquad\qquad \text{for } 0 < \frac{B_0}{m}\Omega \leq \gamma_3; \\
\mathrm{mod}(\Omega t_m, 2\pi) \in (\,\pi, 2\pi\,) \\
\qquad\qquad\qquad\qquad\qquad\quad \text{for } \gamma_3 = 0; \\
\mathrm{mod}(\Omega t_m, 2\pi) \in [\,0, \Theta_3^{\mathrm{cr}}\,) \cup (\,\pi - \Theta_3^{\mathrm{cr}}, 2\pi\,] \\
\qquad \text{for } \gamma_3 < 0 \text{ and } \frac{B_0}{m}\Omega > |\gamma_3|; \\
\mathrm{mod}(\Omega t_m, 2\pi) \in [\,0, \frac{\pi}{2}\,) \cup (\,\frac{\pi}{2}, 2\pi\,] \\
\qquad \text{for } \gamma_3 < 0 \text{ and } \frac{B_0}{m}\Omega = |\gamma_3|; \\
\mathrm{mod}(\Omega t_m, 2\pi) \in [\,0, 2\pi\,] \\
\qquad \text{for } \gamma_3 < 0 \text{ and } \frac{B_0}{m}\Omega < |\gamma_3|,
\end{array}\right\}
\tag{56}
$$

*where*

$$
\Theta_3^{\mathrm{cr}} = \arcsin(-\frac{\gamma_3 m}{B_0 \Omega}),
$$

*and*

$$
\gamma_3 = \frac{c}{m}\ddot{x}_{(2)}(t_m) + \frac{k}{m}\dot{x}_{(2)}(t_m).
$$

(iii) *Suppose the flow in domain $\Omega_2$ reaches $\mathbf{x}_m \in \partial\Omega_{23}$ at time $t_m$, the grazing motion on the boundary $\partial\Omega_{23}$ appears (i.e. the mapping $P_5$ is tangential to the boundary $\partial\Omega_{23}$) iff*

$$
\left.\begin{array}{l}
\mathrm{mod}(\Omega t_m, 2\pi) \in [\,0, \pi + |\Theta_5^{\mathrm{cr}}|\,) \cup (\,2\pi - |\Theta_5^{\mathrm{cr}}|, 2\pi\,] \\
\qquad\qquad\qquad\qquad \text{for } 0 < \gamma_5 < \frac{B_0}{m}\Omega; \\
\mathrm{mod}(\Omega t_m, 2\pi) \in [\,0, \frac{3}{2}\pi\,) \cup (\,\frac{3}{2}\pi, 2\pi\,] \\
\qquad\qquad\qquad\qquad \text{for } 0 < \gamma_5 = \frac{B_0}{m}\Omega; \\
\mathrm{mod}(\Omega t_m, 2\pi) \in [\,0, 2\pi\,] \\
\qquad\qquad\qquad\qquad \text{for } 0 < \frac{B_0}{m}\Omega < \gamma_5; \\
\mathrm{mod}(\Omega t_m, 2\pi) \in (\,0, \pi\,) \\
\qquad\qquad\qquad\qquad\qquad\quad \text{for } \gamma_5 = 0; \\
\mathrm{mod}(\Omega t_m, 2\pi) \in (\,\Theta_5^{\mathrm{cr}}, \pi - \Theta_5^{\mathrm{cr}}\,) \subset (\,0, \pi\,) \\
\qquad \text{for } \gamma_5 < 0 \text{ and } \frac{B_0}{m}\Omega > |\gamma_5|; \\
\mathrm{mod}(\Omega t_m, 2\pi) \in \{\varnothing\} \\
\qquad \text{for } \gamma_5 < 0 \text{ and } \frac{B_0}{m}\Omega < |\gamma_5|,
\end{array}\right\}
\tag{57}
$$

*where*

$$
\Theta_5^{\mathrm{cr}} = \arcsin(-\frac{\gamma_5 m}{B_0 \Omega}),
$$

*and*

$$
\gamma_5 = \frac{c}{m}\ddot{x}_{(2)}(t_m) + \frac{k}{m}\dot{x}_{(2)}(t_m).
$$

(iv) *Suppose the flow in domain $\Omega_3$ reaches $\mathbf{x}_m \in \partial\Omega_{32}$ at time $t_m$, the grazing motion on the boundary $\partial\Omega_{32}$ appears (i.e. the mapping $P_6$ is tangential to the boundary $\partial\Omega_{32}$) iff*

$$
\left.\begin{array}{l}
\mathrm{mod}(\Omega t_m, 2\pi) \in (\,\pi + |\Theta_6^{\mathrm{cr}}|, 2\pi - |\Theta_6^{\mathrm{cr}}|\,) \subset (\,\pi, 2\pi) \\
\qquad\qquad\qquad\qquad \text{for } 0 < \gamma_6 < \frac{B_0}{m}\Omega; \\
\mathrm{mod}(\Omega t_m, 2\pi) \in \{\varnothing\} \\
\qquad\qquad\qquad\qquad \text{for } 0 < \frac{B_0}{m}\Omega \leq \gamma_6; \\
\mathrm{mod}(\Omega t_m, 2\pi) \in (\,\pi, 2\pi\,) \\
\qquad\qquad\qquad\qquad\qquad\quad \text{for } \gamma_6 = 0; \\
\mathrm{mod}(\Omega t_m, 2\pi) \in [\,0, \Theta_6^{\mathrm{cr}}\,) \cup (\,\pi - \Theta_6^{\mathrm{cr}}, 2\pi\,] \\
\qquad \text{for } \gamma_6 < 0 \text{ and } \frac{B_0}{m}\Omega > |\gamma_6|; \\
\mathrm{mod}(\Omega t_m, 2\pi) \in [\,0, \frac{\pi}{2}\,) \cup (\,\frac{\pi}{2}, 2\pi\,] \\
\qquad \text{for } \gamma_6 < 0 \text{ and } \frac{B_0}{m}\Omega = |\gamma_6|; \\
\mathrm{mod}(\Omega t_m, 2\pi) \in [\,0, 2\pi\,] \\
\qquad \text{for } \gamma_6 < 0 \text{ and } \frac{B_0}{m}\Omega < |\gamma_6|,
\end{array}\right\}
\tag{58}
$$

*where*

$$
\Theta_6^{\mathrm{cr}} = \arcsin(-\frac{\gamma_6 m}{B_0 \Omega}),
$$

*and*

$$
\gamma_6 = \frac{c}{m}\ddot{x}_{(3)}(t_m) + \frac{k}{m}\dot{x}_{(3)}(t_m).
$$

**Proof:** (i) For the double-belt friction oscillator described in Section 2, by Theorem 6, the grazing motion conditions for the flow $\mathbf{x}_{(1)}(t)$ in domain $\Omega_1$ on the boundary $\partial\Omega_{12}$ at time $t_m$ are given as

$$
F_{(1)}(\mathbf{x}_m, t_{m\pm}) = 0,
\tag{59}
$$

$$
\nabla F_{(1)}(\mathbf{x}_m, t_{m\pm}) \cdot \mathbf{F}_{(1)}(\mathbf{x}_m, t_{m\pm}) + \frac{\partial F_{(1)}(\mathbf{x}_m, t_{m\pm})}{\partial t_m} < 0.
\tag{60}
$$

With (9), the Eqs. (59) and (60) can be computed as

$$
-\frac{c}{m}\dot{x}_{(1)}(t_m) - \frac{k}{m}x_{(1)}(t_m) + \frac{B_0}{m}\cos\Omega t_m
$$
$$
+\frac{1}{m}[A_0 + (\mu_1 + \mu_2)F_N] = 0,
\tag{61}
$$

$$
-\frac{c}{m}\ddot{x}_{(1)}(t_m) - \frac{k}{m}\dot{x}_{(1)}(t_m) - \frac{B_0\Omega}{m}\sin\Omega t_m < 0.
\tag{62}
$$

The grazing conditions are computed through (54), (61) and (62). Three equations and an inequality have four unknowns, then one unknown must be given.

From (62), the critical value for $\mathrm{mod}(\Omega t_m, 2\pi)$ is introduced through

$$
\Theta_2^{\mathrm{cr}} = \arcsin(-\frac{\gamma_2 m}{B_0 \Omega}),
$$

where $\gamma_2 = \frac{c}{m}\ddot{x}_{(1)}(t_m) + \frac{k}{m}\dot{x}_{(1)}(t_m)$, and the superscript "cr" represents a critical value relative to grazing.

If $0 < \gamma_2 < \frac{B_0}{m}\Omega$, then $-1 < -\frac{\gamma_2 m}{B_0 \Omega} < 0$, we have

$$\mathrm{mod}(\Omega t_m, 2\pi) \in [\,0, \pi + |\Theta_2^{\mathrm{cr}}|\,) \cup (\,2\pi - |\Theta_2^{\mathrm{cr}}|, 2\pi\,].$$

If $0 < \gamma_2 = \frac{B_0}{m}\Omega$, then $-\frac{\gamma_2 m}{B_0 \Omega} = -1$, we have

$$\mathrm{mod}(\Omega t_m, 2\pi) \in [\,0, \frac{3}{2}\pi\,) \cup (\,\frac{3}{2}\pi, 2\pi\,].$$

If $0 < \frac{B_0}{m}\Omega < \gamma_2$, then $-\frac{\gamma_2 m}{B_0 \Omega} < -1$, we have

$$\mathrm{mod}(\Omega t_m, 2\pi) \in [\,0, 2\pi\,].$$

If $\gamma_2 = 0$, then $-\frac{\gamma_2 m}{B_0 \Omega} = 0$, we have

$$\mathrm{mod}(\Omega t_m, 2\pi) \in (\,0, \pi\,).$$

If $\gamma_2 < 0$ and $\frac{B_0}{m}\Omega > |\gamma_2|$, then $0 < -\frac{\gamma_2 m}{B_0 \Omega} < 1$, we have

$$\mathrm{mod}(\Omega t_m, 2\pi) \in (\,\Theta_2^{\mathrm{cr}}, \pi - \Theta_2^{\mathrm{cr}}\,) \subset (\,0, \pi\,).$$

If $\gamma_2 < 0$ and $\frac{B_0}{m}\Omega < |\gamma_2|$, then $-\frac{\gamma_2 m}{B_0 \Omega} > 1$, we have

$$\mathrm{mod}(\Omega t_m, 2\pi) \in \{\varnothing\}.$$

Therefore (i) holds;

(ii) Similarly, for the double-belt friction oscillator described in Section 2, by Theorem 6, the grazing motion conditions for the flow $\mathbf{x}_{(2)}(t)$ in domain $\Omega_2$ on the boundary $\partial\Omega_{21}$ at time $t_m$ are given as

$$F_{(2)}(\mathbf{x}_m, t_{m\pm}) = 0, \qquad (63)$$

$$\nabla F_{(2)}(\mathbf{x}_m, t_{m\pm}) \cdot \mathbf{F}_{(2)}(\mathbf{x}_m, t_{m\pm}) + \frac{\partial F_{(2)}(\mathbf{x}_m, t_{m\pm})}{\partial t_m} > 0. \qquad (64)$$

With (9), the Eqs. (63) and (64) can be computed as

$$-\frac{c}{m}\dot{x}_{(2)}(t_m) - \frac{k}{m}x_{(2)}(t_m) + \frac{B_0}{m}\cos\Omega t_m$$
$$+ \frac{1}{m}[A_0 - (\mu_1 - \mu_2)F_N] = 0, \qquad (65)$$

$$-\frac{c}{m}\ddot{x}_{(2)}(t_m) - \frac{k}{m}\dot{x}_{(2)}(t_m) - \frac{B_0 \Omega}{m}\sin\Omega t_m > 0. \qquad (66)$$

The grazing conditions are computed through (54), (65) and (66). Three equations and an inequality have four unknowns, then one unknown must be given.

From (66), the critical value for $\mathrm{mod}(\Omega t_m, 2\pi)$ is introduced through

$$\Theta_3^{\mathrm{cr}} = \arcsin\!\left(-\frac{\gamma_3 m}{B_0 \Omega}\right),$$

where $\gamma_3 = \frac{c}{m}\ddot{x}_{(2)}(t_m) + \frac{k}{m}\dot{x}_{(2)}(t_m)$, and the superscript "cr" represents a critical value relative to grazing.

If $0 < \gamma_3 < \frac{B_0}{m}\Omega$, then $-1 < -\frac{\gamma_3 m}{B_0 \Omega} < 0$, we have

$$\mathrm{mod}(\Omega t_m, 2\pi) \in (\,\pi + |\Theta_3^{\mathrm{cr}}|, 2\pi - |\Theta_3^{\mathrm{cr}}|\,) \subset (\,\pi, 2\pi\,).$$

If $0 < \frac{B_0}{m}\Omega \leq \gamma_3$, then $-\frac{\gamma_3 m}{B_0 \Omega} \leq -1$, we have

$$\mathrm{mod}(\Omega t_m, 2\pi) \in \{\varnothing\}.$$

If $\gamma_3 = 0$, then $-\frac{\gamma_3 m}{B_0 \Omega} = 0$, we have

$$\mathrm{mod}(\Omega t_m, 2\pi) \in (\,\pi, 2\pi\,).$$

If $\gamma_3 < 0$ and $\frac{B_0}{m}\Omega > |\gamma_3|$, then $0 < -\frac{\gamma_3 m}{B_0 \Omega} < 1$, we have

$$\mathrm{mod}(\Omega t_m, 2\pi) \in [\,0, \Theta_3^{\mathrm{cr}}\,) \cup (\,\pi - \Theta_3^{\mathrm{cr}}, 2\pi\,].$$

If $\gamma_3 < 0$ and $\frac{B_0}{m}\Omega = |\gamma_3|$, then $-\frac{\gamma_3 m}{B_0 \Omega} = 1$, we have

$$\mathrm{mod}(\Omega t_m, 2\pi) \in [\,0, \frac{\pi}{2}\,) \cup (\,\frac{\pi}{2}, 2\pi\,].$$

If $\gamma_3 < 0$ and $\frac{B_0}{m}\Omega < |\gamma_3|$, then $-\frac{\gamma_3 m}{B_0 \Omega} > 1$, we have

$$\mathrm{mod}(\Omega t_m, 2\pi) \in [\,0, 2\pi\,].$$

Therefore (ii) holds.

Similarly we can prove that (iii) and (iv) hold. □

# 6 Numerical Simulations

To verify the analytical conditions of the stick motions and grazing motions obtained in Section 4 and Section 5, the motions of the mass in the double-belt friction oscillator will be demonstrated through the time histories of displacement and velocity, the corresponding trajectory of the mass in phase space. In this section, the force product will be presented to illustrate the starting and vanishing points of stick motions. The displacements or the velocities of the belt 1 and belt 2 are presented by black curves, and the displacement or the velocity of the mass, the corresponding trajectories of the motions of the mass in phase space are presented by red curves. The onset points of stick or periodic motions are marked by blue-solid circular symbols, the vanishing points of stick or periodic motions are marked by green-solid circular symbols, the switching points are depicted by red-solid circular symbols.

Consider the system parameters as $A_0 = -15, B_0 = 10, \Omega = 1, c = 1, k = 1, m = 1, g = 9.81, v_1 = 1, v_2 = 5, \mu_1 = 0.8, \mu_2 = 0.6, F_N = 9.81$ to demonstrate a stick motion of the mass on
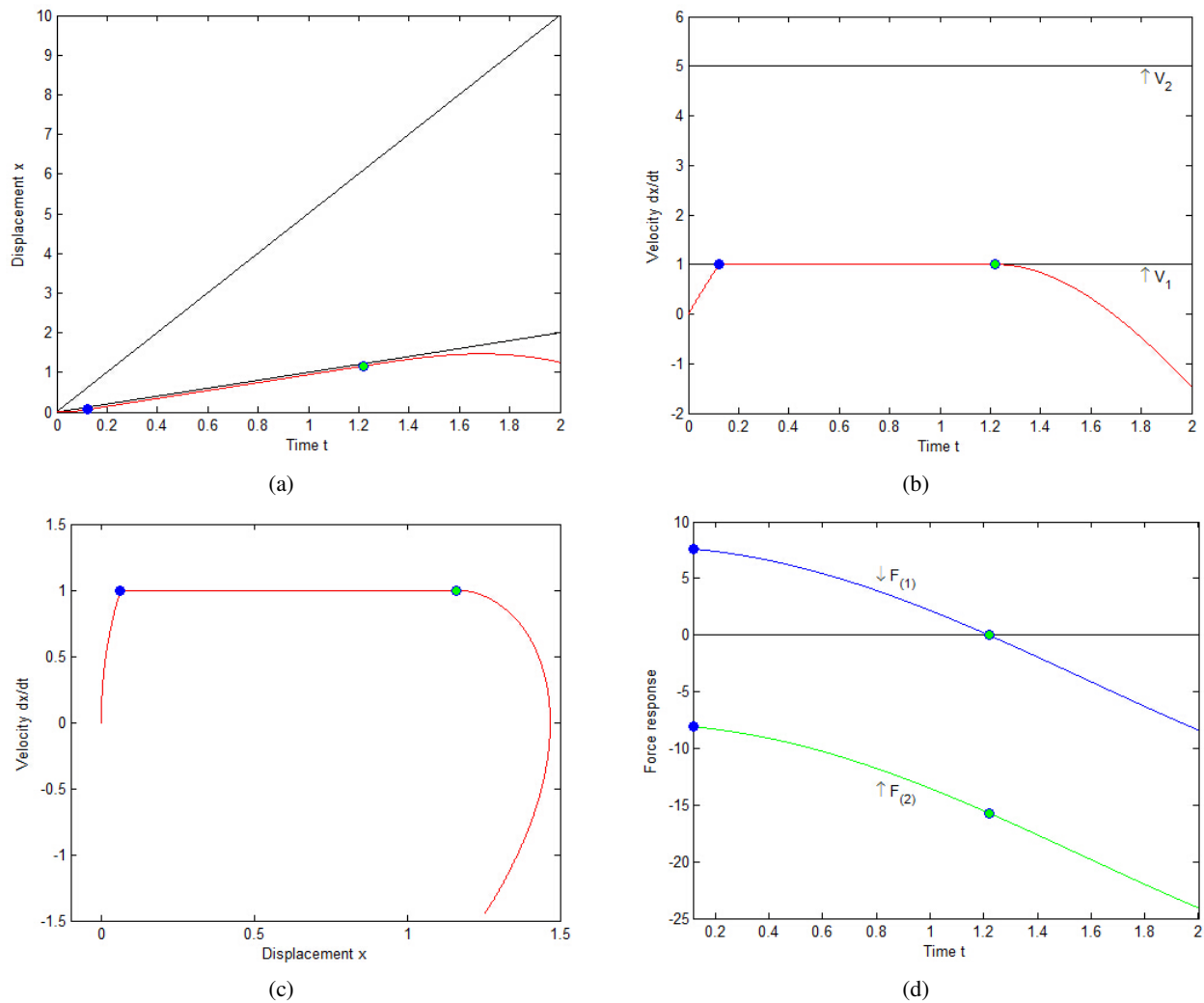
Figure 5: Numerical simulation of a stick motion on the boundary $\partial\Omega_{12}$: (a) displacement-time history, (b) velocity-time history, (c) phase trajectory, (d) force-time history. ($A_0 = -15, B_0 = 10, \Omega = 1, c = 1, k = 1, m = 1, g = 9.81, v_1 = 1, v_2 = 5, \mu_1 = 0.8, \mu_2 = 0.6, F_N = 9.81, t_0 = 0, x_0 = 0, \dot{x}_0 = 0$).

the boundary $\partial\Omega_{12}$. The initial conditions are $t_0 = 0, x_0 = 0, \dot{x}_0 = 0$. For a better understanding of mechanism of stick motions, the time-history responses for displacement, velocity, the corresponding trajectory and force response will be illustrated. The time histories of displacement and velocity are shown in Fig. 5(a) and (b), respectively. With the initial conditions $t_0 = 0, x_0 = 0, \dot{x}_0 = 0$, the stick motion of the belt 1 appears after a period of time. The blue-solid circular symbol represents the onset point of the stick motion. It can be seen that the velocity of the mass is equal to the speed of the belt 1, and then the mass and the belt 1 move together for some time. During this time, the mass and the belt 1 have the same displacement increase. The green-solid circular symbol represents the vanishing point of the stick motion. After vanishing of stick motion on the boundary $\partial\Omega_{12}$, the mass moves under the influence of friction force.

In Fig. 5(c), the corresponding trajectory of the stick motion on the boundary $\partial\Omega_{12}$ is plotted. Further, the force-time histories are also presented in Fig. 5(d). The blue curve stands for $F_{(1)}$ and the green curve stands for $F_{(2)}$. Between the blue-solid circular symbol and the green-solid circular symbol, it is observed that $F_{(1)} > 0$ and $F_{(2)} < 0$. This satisfy the analytical conditions of the stick motion on the boundary $\partial\Omega_{12}$ described in Theorem 4. After vanishing of the stick motion, $F_{(1)} \times F_{(2)} > 0$.

Consider a stick motion on the boundary $\partial\Omega_{23}$ with the system parameters $A_0 = 5, B_0 = 10, \Omega = 0.1, c = 1, k = 1, m = 1, g = 9.81, v_1 = 1, v_2 = 5, \mu_1 = 0.8, \mu_2 = 0.6, F_N = 9.81$. The time-history responses for displacement, velocity, the corresponding trajectory and force response of such a stick motion are illustrated in Fig. 6. The initial conditions $t_0 = 0, x_0 = 0, \dot{x}_0 = 5$ are selected to make the stick
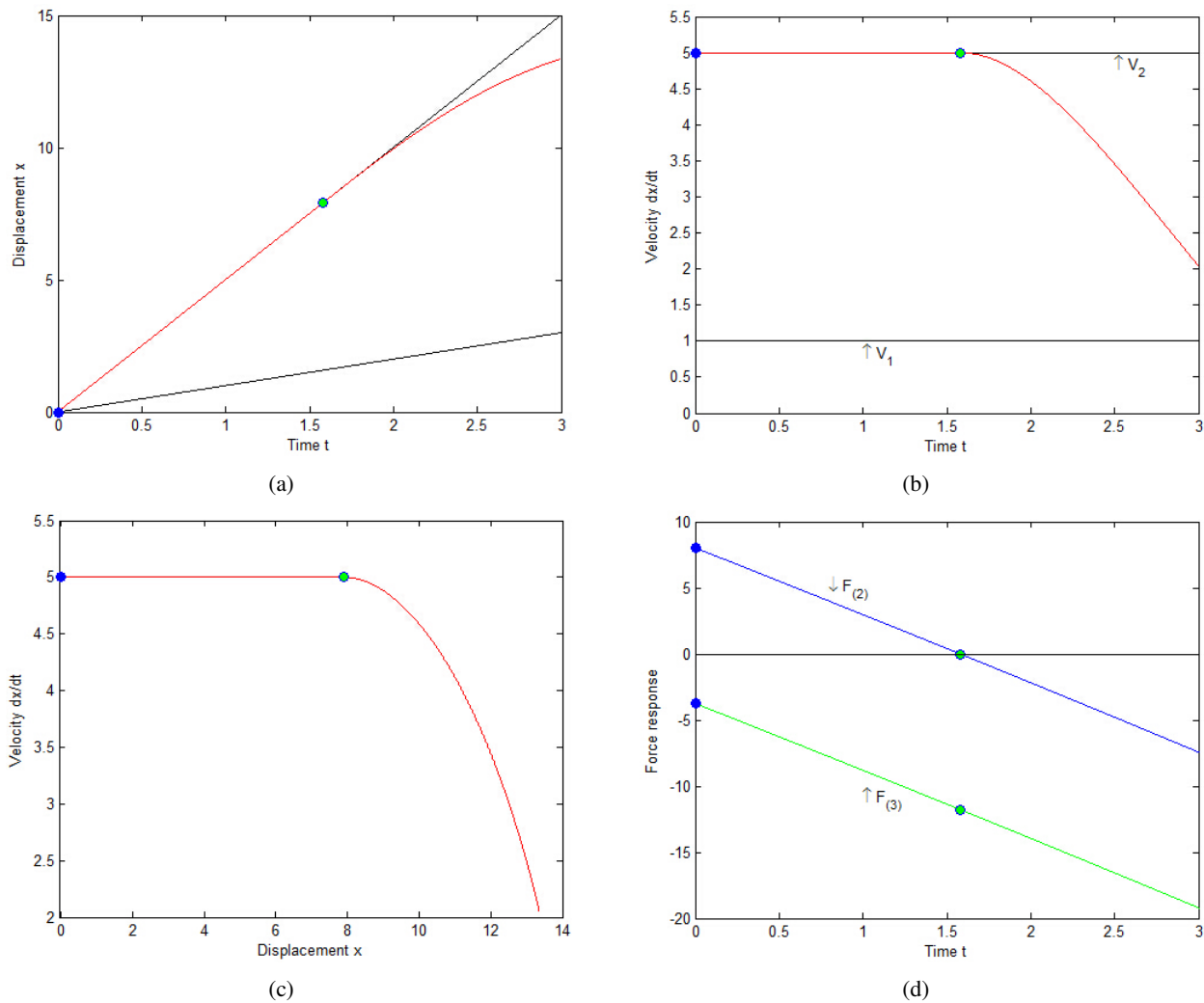
Figure 6: Numerical simulation of a stick motion on the boundary $\partial\Omega_{23}$ : (a) displacement-time history, (b) velocity-time history, (c) phase trajectory, (d) force-time history. ($A_0 = 5, B_0 = 10, \Omega = 0.1, c = 1, k = 1, m = 1, g = 9.81, v_1 = 1, v_2 = 5, \mu_1 = 0.8, \mu_2 = 0.6, F_N = 9.81, t_0 = 0, x_0 = 0, \dot{x}_0 = 5$).

motion on the boundary $\partial\Omega_{23}$ appear in such initial conditions. The blue-solid circular symbol and the green-solid circular symbol represent the onset and vanishing points of the stick motion, respectively. In Fig. 6(a) and (b), the curves between the blue-solid circular symbol and the green-solid circular symbol are the intersection between the black curve and the red one. In this period, the mass and the belt 2 moves together and have the same velocity and displacement. The corresponding trajectory of the stick motion on the boundary $\partial\Omega_{23}$ is presented in Fig. 6(c). After the vanishing of the stick motion, the trajectory of the mass in the phase plane exists in domain $\Omega_2$ for some time. The force-time histories are also plotted in In Fig. 6(d). The blue curve stands for $F_{(2)}$ and the green curve stands for $F_{(3)}$. It is observed that the stick motion on the boundary $\partial\Omega_{23}$ satisfy $F_{(2)} > 0$ and $F_{(3)} < 0$. At the green-solid circular symbol,

$F_{(2)} = 0$ and $F_{(3)} < 0$. Then the stick motion vanishes.

The system parameters $A_0 = 5, B_0 = 10, \Omega = 1, c = 2, k = 2, m = 1, g = 9.81, v_1 = 5, v_2 = 10, \mu_1 = 0.7, \mu_2 = 0.2, F_N = 9.81$ are chosen to illustrate a grazing motion of mapping $P_2$ in domain $\Omega_1$. The initial conditions are $t_0 = 2.5, x_0 = -3.1049, \dot{x}_0 = 1.3369$. In Fig. 7(b) and (c), the time history responses for velocity of such a grazing motion are presented. In Fig. 7(b), it is clear that the velocity of the mass is equal to the belt 1 at the red point only. It means that the motion is tangential to the velocity boundary $\partial\Omega_{12}$ and then leaves this boundary again, so the red point is grazing point. The blue point stands for the start point of a simple periodic motion. At the green point, the first period finishes and the next period begins. The periodicity of this simple periodic motion can be seen clearly in Fig.
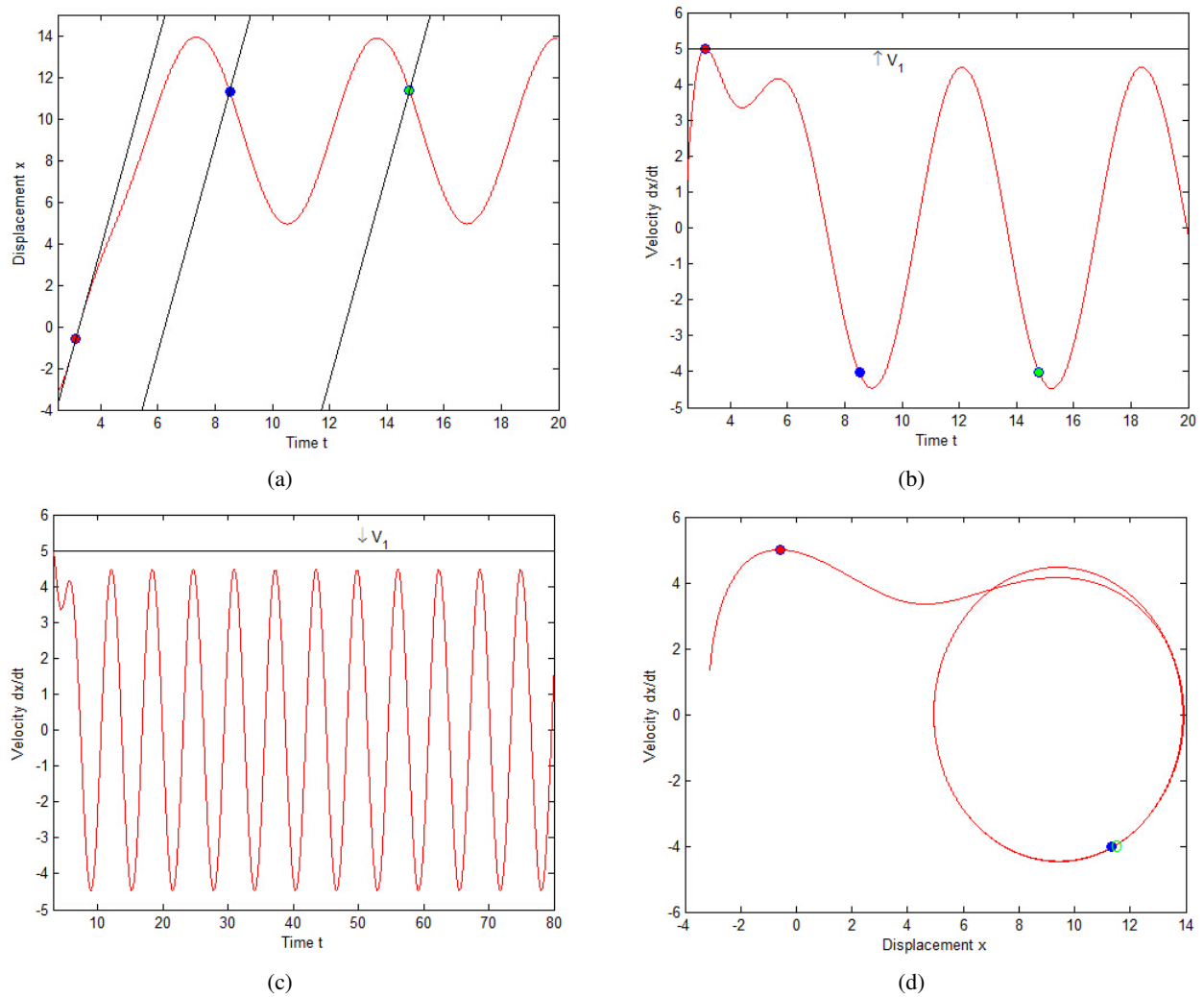
(a)



(b)



(c)



(d)

Figure 7: Numerical simulation of a grazing motion of mapping $P_2$ in domain $\Omega_1$ : (a) displacement-time history, (b) velocity-time history, (c) velocity-time history for multiple period, (d) phase trajectory. ($A_0 = 5, B_0 = 10, \Omega = 1, c = 2, k = 2, m = 1, g = 9.81, v_1 = 5, v_2 = 10, \mu_1 = 0.7, \mu_2 = 0.2, F_N = 9.81, t_0 = 2.5, x_0 = -3.1049, \dot{x}_0 = 1.3369$).

7(c). The time history response for displacement of such a grazing motion is plotted in Fig. 7(a). Three black curves in Fig. 7(a) represent the displacement of special points on the belt 1, such as the grazing point, the start and end points of the first period. It can be observed that the red point is the intersection between the black curve and the red one, so at the red point, the mass and the grazing point have the same displacement and velocity. However, at the blue and green points, the mass and the blue or green point only have the same displacement, the velocities of them are not equal, so the blue and green points are not grazing point. In phase plane, the trajectory of the grazing motion is tangential to the velocity boundary $\partial\Omega_{12}$ in domain $\Omega_1$, as shown in Fig. 7(d). In phase plane, the blue point and the green point are the same point.

The system parameters $A_0 = 10, B_0 = 16, \Omega = 2, c = 4, k = 8, m = 2, g = 9.81, v_1 = -4, v_2 = 4, \mu_1 = 0.8, \mu_2 = 0.5, F_N = 19.62$ and the initial conditions $t_0 = 2.5, x_0 = 5.8980, \dot{x}_0 = 2.2580$ are given to demonstrate the grazing motion of mapping $P_3$ in domain $\Omega_2$ in Fig. 8. The history of velocity of the grazing motion is shown in Fig. 8(b). It can be seen that the velocity of the mass is equal to the belt 1 at the red point and then leaves this velocity boundary again. It means that the motion is tangential to the velocity boundary $\partial\Omega_{21}$, so the red point is grazing point. After the grazing motion, the velocity of the mass reaches the velocity boundary again at the blue point. More detailed illustration is shown in Fig. 8(c). At the points between the blue point and the green point, the force response satisfy $F_{(1)} > 0$ and
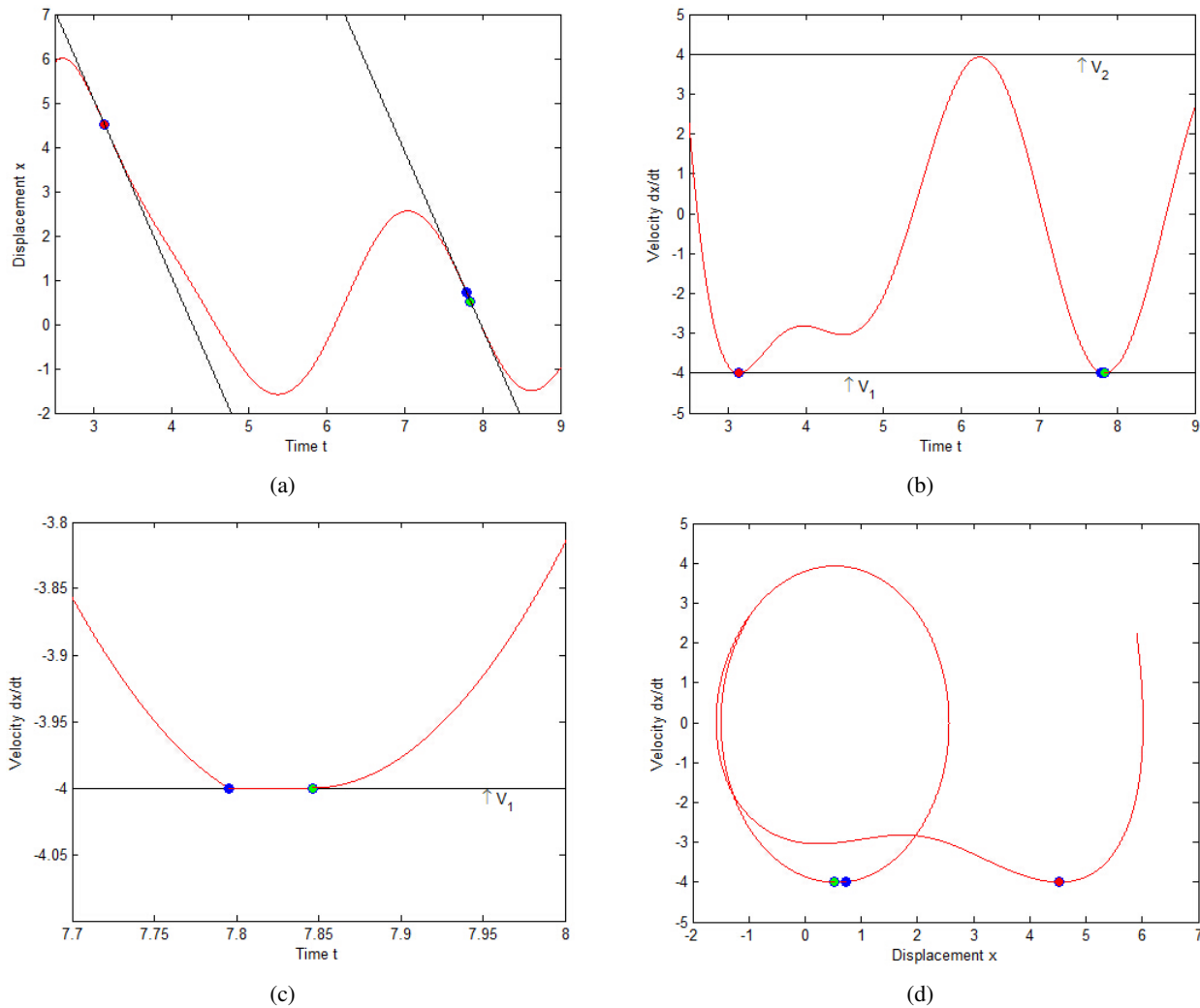
Figure 8: Numerical simulation of a grazing motion of mapping $P_3$ in domain $\Omega_2$ : (a) displacement-time history, (b) velocity-time history, (c) velocity-time history, (d) phase trajectory. ($A_0 = 10, B_0 = 16, \Omega = 2, c = 4, k = 8, m = 2, g = 9.81, v_1 = -4, v_2 = 4, \mu_1 = 0.8, \mu_2 = 0.5, F_N = 19.62, t_0 = 2.5, x_0 = 5.8980, \dot{x}_0 = 2.2580$).

$F_{(2)} < 0$. Then the stick motion appears in such conditions, and the mass moves together with the belt 1. The blue and the green points stand for the onset and the vanishing points of the stick motion, respectively. After the vanishing of stick motion on the belt 1, the velocity of the mass leaves this velocity boundary again. In Fig. 8(a), two black curves represent the history of displacement of the grazing point(or called the red point) and the onset point of stick motion(or called the blue point). The intersection of the red curve and black curves is the red point and the curve between the blue and the green point, stand for the grazing motion and the stick motion, respectively. The trajectory of the grazing motion in domain $\Omega_2$ is shown in Fig. 8(d). It can be observed that the trajectory of the grazing motion in domain $\Omega_2$ is tangential to the velocity boundary $\partial\Omega_{21}$, and the trajectory of the stick motion is a part of the velocity boundary $\partial\Omega_{21}$.

From the basic mappings in Section 5, non-stick and stick periodic motions of the double-belt friction oscillator can be obtained. The following Fig. 9 and Fig. 10 illustrate the non-stick and stick periodic motions, respectively. Also, the time-history responses of displacement, velocity and the corresponding trajectory will be illustrated. Besides, for a better understanding of the mechanisms of non-stick and stick periodic motions, the force responses relative to time, displacement and velocity will be presented, too.

The system parameters $A_0 = -2, B_0 = 9, \Omega = 4, c = 0.2, k = 3, m = 0.1, g = 9.81, v_1 = 1, v_2 = 25, \mu_1 = 0.3, \mu_2 = 0.2, F_N = 10$ are used to illustrate a non-stick periodic motion of mapping $P_{32} = P_3 \circ P_2$. With the initial conditions $t_0 = 0.1324, x_0 = 4.5447, \dot{x}_0 = 1$, numerical simulations can be obtained, as shown in Fig. 9. The time-history responses of displacement, velocity and
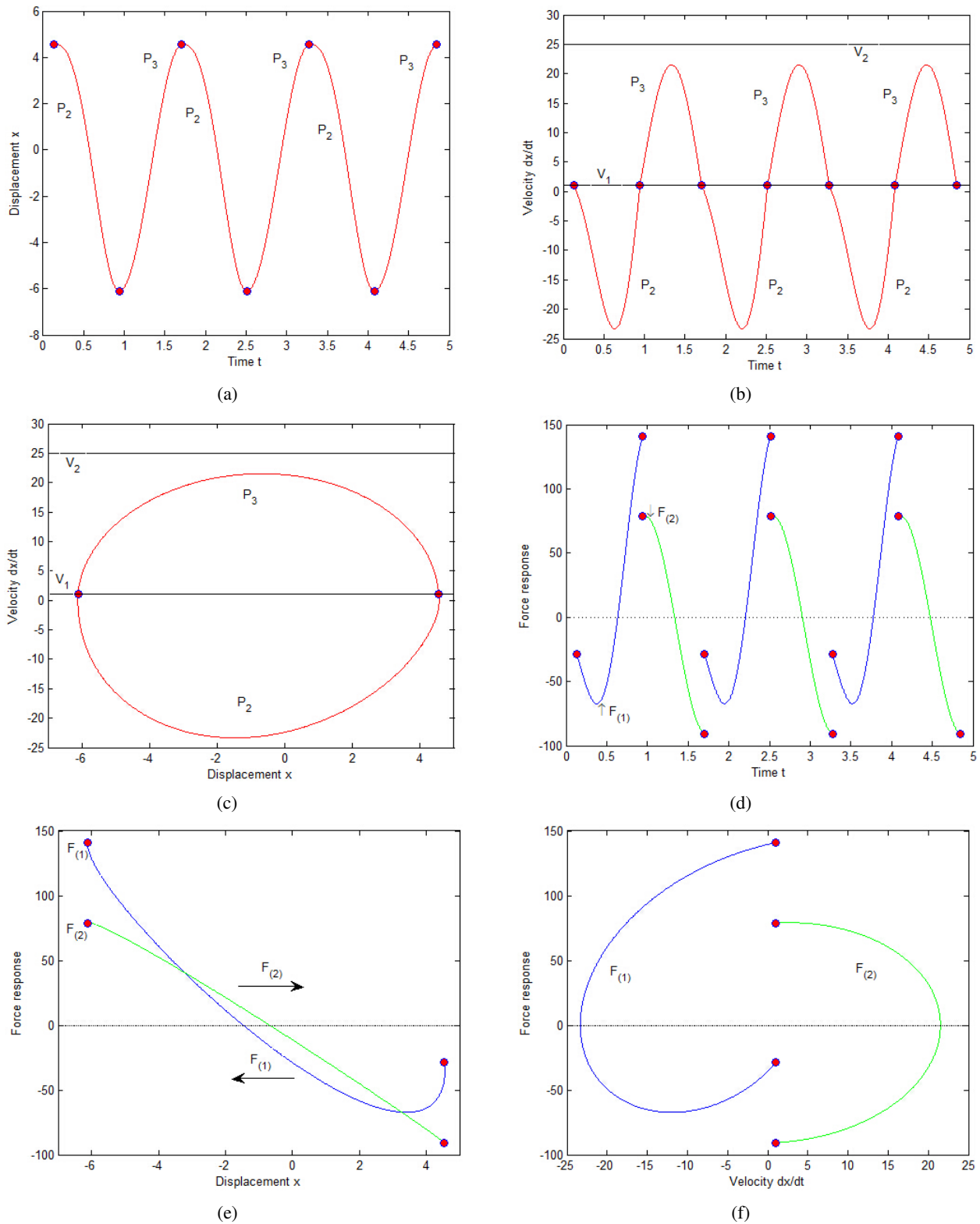
Figure 9: Numerical simulation of a non-stick periodic motion relative to mapping $P_{32} = P_3 \circ P_2$ : (a) displacement-time history, (b) velocity-time history, (c) phase trajectory, (d) force-time history, (e) force-displacement history, (f) force-velocity history ($A_0 = -2, B_0 = 9, \Omega = 4, c = 0.2, k = 3, m = 0.1, g = 9.81, v_1 = 1, v_2 = 25, \mu_1 = 0.3, \mu_2 = 0.2, F_N = 10, t_0 = 0.1324, x_0 = 4.5447, \dot{x}_0 = 1$).
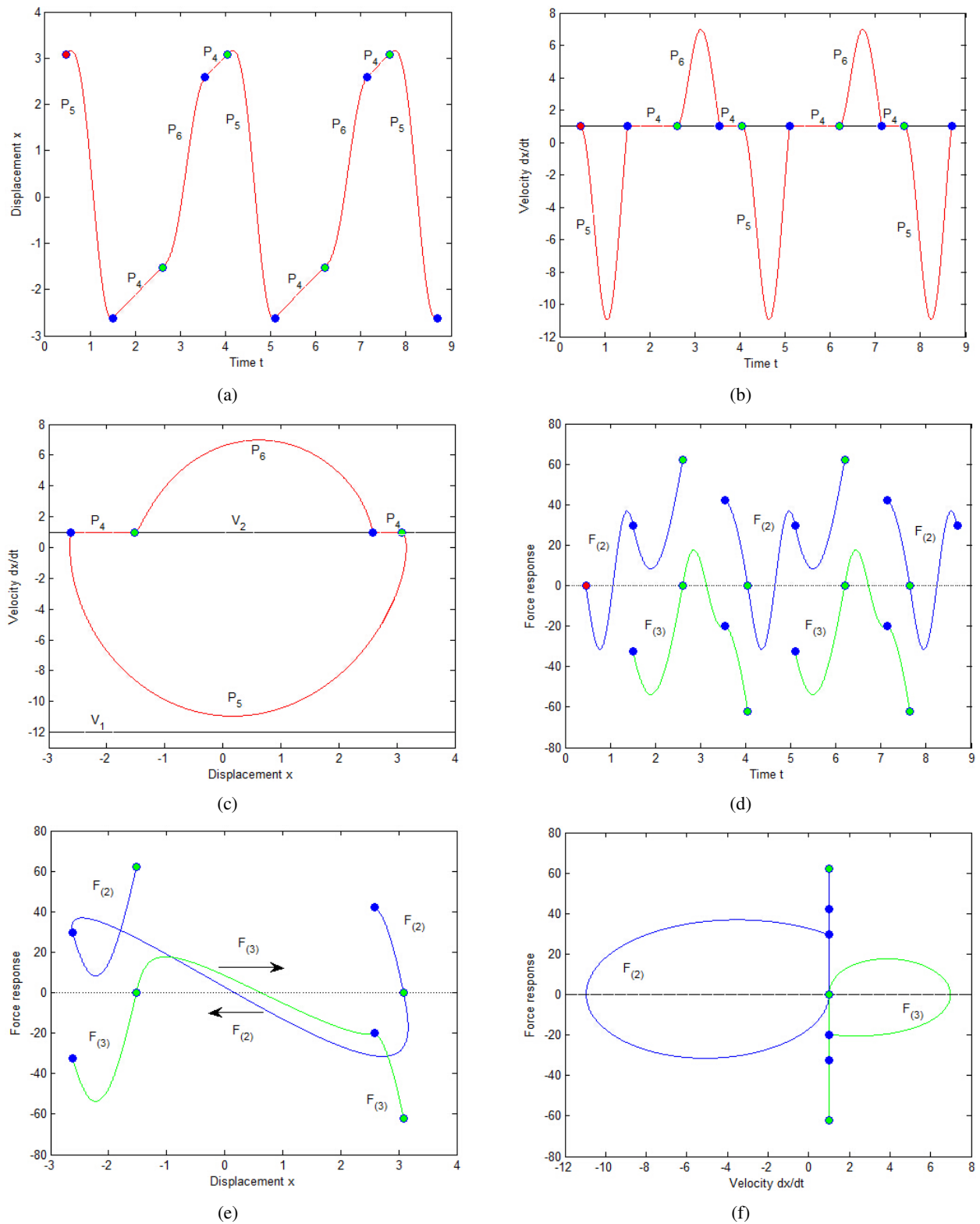
Figure 10: Numerical simulation of a stick periodic motion relative to mapping $P_{4645} = P_4 \circ P_6 \circ P_4 \circ P_5$ : (a) displacement-time history, (b) velocity-time history, (c) phase trajectory, (d) force-time history, (e) force-displacement history, (f) force-velocity history ($A_0 = 5, B_0 = 9, \Omega = 1.75, c = 0.2, k = 3, m = 0.1, g = 9.81, v_1 = -12, v_2 = 1, \mu_1 = 0.5, \mu_2 = 0.3, F_N = 10, t_0 = 0.4588, x_0 = 3.0837, \dot{x}_0 = 1$).

force response for the non-stick periodic motion are plotted in Fig. 9(a), (b) and (d). The blue curve stands for $F_{(1)}$ and the green curve stands for $F_{(2)}$. The switching points are marked by red-solid circular symbols. From Fig. 9(d), it can be observed that $F_{(1)} \times F_{(2)} > 0$ on the red points at the same time. By Theorem 5, the motion will pass through the velocity boundary. Further, the corresponding trajectory in phase plane is presented in Fig. 9(c). Obviously, there is no stick motion exists in Fig. 9(c). The mapping switching from $P_\alpha$ to $P_\beta$ ($\alpha, \beta \in \{2, 3\}$ and $\alpha \neq \beta$) is continuous. The relation between the displacement and force in Fig. 9(e) and the relation between the velocity and force in Fig. 9(f) verifies the criteria in Theorem 5 at the velocity boundary.

The system parameters $A_0 = 5, B_0 = 9, \Omega = 1.75, c = 0.2, k = 3, m = 0.1, g = 9.81, v_1 = -12, v_2 = 1, \mu_1 = 0.5, \mu_2 = 0.3, F_N = 10$ are given to illustrate a stick periodic motion for mapping structures $P_{4645}$. The initial conditions $t_0 = 0.4588, x_0 = 3.0837, \dot{x}_0 = 1$ are selected to make the stick motion on the boundary $\partial\Omega_{23}$ appear in such initial conditions. The time-history responses of displacement, velocity and the corresponding trajectory in phase plane are shown in Fig. 10(a), (b) and (c). The blue-solid circular symbol and the green-solid circular symbol represent the onset and vanishing points of the stick motion, respectively. It is clearly seen that two stick parts( i.e. $P_4$) exist in this periodic motion. The time-history responses of forces for the stick periodic motion are plotted in Fig. 10(d), the blue curve stands for $F_{(2)}$ and the green curve stands for $F_{(3)}$. Obviously, on the blue points at the same time we have $F_{(2)} \times F_{(3)} < 0$, then the stick motion on the boundary $\partial\Omega_{23}$ appears. However, at the green points at the same time we have $F_{(2)} \times F_{(3)} = 0$. It means the vanishing of the stick motion and the beginning of non-stick motion. In Fig. 10(e) and (f), the relations between the force and displacement or velocity are presented. These can help us to understand the mechanisms of stick periodic motion relative to displacement and velocity.

# 7   Conclusion

This paper was concerned with the dynamics of a double belt friction oscillator which was subjected to periodic excitation, linear spring-loading, damping force and two friction forces using the flow switchability theory of the discontinuous dynamical systems. Different domains and boundaries for such system were defined according to the friction discontinuity, which exhibited multiple discontinuous boundaries in the phase space. Based on the above domains and boundaries, the analytical conditions of the stick motions,

grazing motions and periodic motions were obtained mathematically. The numerical simulations were given to illustrate the analytical results of these motions.

⋆ Corresponding author: Jinjun Fan.

E-mail: fjj18@126.com(J.Fan).

*References:*

[1] J.P. Den Hartog, Forced vibrations with Coulomb and viscous damping, *Transactions of the American Society of Mechanical Engineers* 53, 1930, pp. 107–115.

[2] E.S. Levitan, Forced oscillation of a spring-mass system having combined Coulomb and viscous damping, *Journal of the Acoustical Society of America* 32, 1960, pp.1265-1269.

[3] S.F. Masri, T.D. Caughey, On the stability of the impact damper, *ASME Journal of Applied Mechanics* 33, 1966, pp.586-592.

[4] S.F. Masri, General motion of impact dampers, *Journal of the Acoustical Society of America* 47, 1970, pp.229-237.

[5] V.I. Utkin, Variable structure systems with sliding modes, *IEEE Transactions on Automatic Control* 22, 1976, pp.212-222.

[6] V.I. Utkin, Sliding modes and their application in variable structure systems, *Moscow:Mir* 1978

[7] V.I. Utkin, Sliding regimes in optimization and control problem, *Moscow: Nauka* 1981

[8] S.W. Shaw, On the dynamical response of a system with dry-friction, *Journal of Sound and Vibration* 108, 1986, pp.305-325.

[9] A.F. Filippov, Differential Equations with Discontinuous Righthand Sides, *Kluwer Academic Publishers,* Dordrecht–Boston–London 1988.

[10] R.I. Leine, D.H. Van Campen, A.De. Kraker, L. Van Den Steen, Stick-slip vibration induced by alternate friction models, *Nonlinear Dynamics* 16, 1998, pp.41-54.

[11] U. Galvanetto, S.R. Bishop, Dynamics of a simple damped oscillator undergoing stick-slip vibrations, *Meccanica* 34, 1999, pp.337-347.

[12] V.N. Pilipchuk, C.A. Tan, Creep-slip capture as a possible source of squeal during decelerating sliding, *Nonlinear Dynamics* 35, 2004, pp.258-285.

[13] P. Casini, F. Vestroni, Nonsmooth dynamics of a double-belt friction oscillator, *IUTAM Symposium on Chaotic Dynamics and Control of Systems and Processes in Mechanics*, 2005, pp.253-262.

[14] A.C.J. Luo, A theory for non-smooth dynamical systems on connectable domains, *Communication in Nonlinear Science and Numerical Simulation* 10, 2005, pp.1-55.

[15] A.C.J. Luo, Imaginary, sink and source flows in the vicinity of the separatrix of nonsmooth dynamic system, *Journal of Sound and Vibration* 285, 2005, pp.443-456.

[16] A.C.J. Luo, Singularity and Dynamics on Discontinuous Vector Fields, *Amsterdam: Elsevier* 2006

[17] A.C.J. Luo, A theory for flow swtichability in discontinuous dynamical systems, *Nonlinear Analysis: Hybrid Systems* 2, 2008, pp.1030-1061.

[18] A.C.J. Luo, Discontinuous Dynamical Systems on Time-varying Domains, Higher Education Press, Beijing China 2009.

[19] A.C.J. Luo, Discontinuous Dynamical Systems, Higher Education Press, Beijing and Springer-Verlag Berlin Heidelberg 2012.

[20] A.C.J. Luo, B.C. Gegg, On the mechanism of stick and non-stick periodic motion in a forced oscillator including dry-friction, *ASME Journal of Vibration and Acoustics* 128, 2006, pp.97-105.

[21] A.C.J. Luo, B.C. Gegg, Stick and non-stick periodic motions in a periodically forced,linear oscillator with dry friction, *Journal of Sound and Vibration* 291, 2006, pp.132-168.

[22] A.C.J. Luo, S. Thapa, Periodic motions in a simplified brake dynamical system with a periodic excitation, *Communication in Nonlinear Science and Numerical Simulation* 14, 2008, pp.2389-2412.

[23] A.C.J. Luo, Fuhong Min, Synchronization of a periodically forced Duffing oscillator with a periodically excited pendulum, *Nonlinear Analysis: Real World Applications* 12, 2011, pp.1810-1827.

[24] A.C.J. Luo, Jianzhe Huang, Discontinuous dynamics of a non-linear, self-excited, friction-induced, periodically forced oscillator, *Nonlinear Analysis: Real World Applications* 13, 2012, pp.241-257.

[25] Yanyan Zhang, Xilin Fu, On periodic motions of an inclined impact pair, *Commun Nonlinear Sci Numer Simulat* 20, 2015, pp.1033-1042.

[26] Xilin Fu, Yanyan Zhang, Stick motions and grazing flows in an inclined impact oscillator, *Chaos, Solitons & Fractals* 76, 2015, pp.218-230.